

G. MRÓWKA-NOWOTNIK*

EXAMINATION OF INTERMETALLIC PHASES IN $\text{AlCu}_4\text{Ni}_2\text{Mg}_2$ ALUMINIUM ALLOY IN T6 CONDITION

ANALIZA FAZ MIĘDZYMETALICZNYCH W STOPIE ALUMINIUM $\text{AlCu}_4\text{Ni}_2\text{Mg}_2$ W STANIE T6

In the technical Al alloys even small quantity of the impurities like Fe and Mn causes the formation of new phases. The particles of intermetallic phases form either on solidification or whilst the alloy is at a relatively high temperature in the solid state, e.g. during homogenization, solution treatment or recrystallization. The exact composition of the alloy and casting conditions will directly influence the type and volume fraction of intermetallic phases. The main objective of this study was to analyze the morphology and composition of the complex microstructure of intermetallic phases in the cast $\text{AlCu}_4\text{Ni}_2\text{Mg}_2$ aluminium alloy in T6 condition. Several techniques: optical light microscopy (LM), transmission (TEM) and scanning (SEM) electron microscopy combined with an energy dispersive X-ray microanalysis (EDS), X-ray diffraction (XRD) were used to identify intermetallics in the $\text{AlCu}_4\text{Ni}_2\text{Mg}_2$ aluminum alloy. This article also briefly reviews the competitive chemical method developed for extracting the second-phase particles from the examined alloy. The results of chemical boiling phenol extraction technique have been compared with the data obtained by the usual metallographic techniques. The results show that the microstructure of cast alloy in T6 condition contains a wide range of intermetallic phases. The following phases were identified and described: θ' - Al_2Cu , Al_6Fe , $\text{Al}_7\text{Cu}_4\text{Ni}$, Al_2CuMg , $\text{Al}_3(\text{CuFeNi})_2$.

W technicznych stopach aluminium nawet niewielka zawartość zanieczyszczeń np.: Fe i Mn powoduje tworzenie się faz międzymetalicznych. Wydzielenia faz międzymetalicznych mogą powstawać podczas krzepnięcia lub kiedy stop poddany jest wysokotemperaturowej obróbce cieplnej, np.: podczas wyżarzania ujednorodniającego, przesycań czy rekrytalizacji. Bezpośredni wpływ na rodzaj oraz objętość względną wydzieleni faz międzymetalicznych w stopach aluminium ma skład chemiczny stopów oraz warunki prowadzenia procesu odlewania. Celem głównym pracy była analiza złożonej mikrostruktury - morfologii oraz składu fazowego, odlewniczego stopu aluminium $\text{AlCu}_4\text{Ni}_2\text{Mg}_2$ po obróbce cieplnej T6. W celu zidentyfikowania faz międzymetalicznych w badanym stopie zastosowano wiele metod i technik badawczych m.in.: mikroskopię świetlną (LM), transmisyjną (TEM) i skaningową (SEM) mikroskopię elektronową z mikroanalizatorem EDS oraz rentgenowską analizę fazową (XRD). W niniejszej pracy zastosowano - obok metod metalograficznych, izolację cząsteczek faz międzymetalicznych przy użyciu wrzącego fenolu. Wyniki analizy proszku zawierającego fazy międzymetaliczne uzyskanego w procesie izolacji porównano z wynikami uzyskanymi przy zastosowaniu standardowych metod badań metalograficznych. Uzyskane wyniki badań pozwoliły zidentyfikować w mikrostrukturze stopu $\text{AlCu}_4\text{Ni}_2\text{Mg}_2$ w stanie T6 następujące fazy międzymetaliczne: θ' - Al_2Cu , Al_6Fe , $\text{Al}_7\text{Cu}_4\text{Ni}$, Al_2CuMg oraz $\text{Al}_3(\text{CuFeNi})_2$.

1. Introduction

Commercial aluminium alloys contains a number of second-phase particles, some of which are present because of deliberate alloying additions and others arising from common impurity elements and their interactions. Coarse intermetallic particles are formed during solidification – in the interdendritic regions, or whilst the alloy is at a relatively high temperature in the solid state, for example, during homogenization, solution treatment or recrystallization [1-20]. They usually contain Fe and other alloying elements and/or impurities. In the aluminium

alloys besides the alloying elements, transition metals such as Fe, Mn and Cr are always present. Even not a large amount of these impurities causes the formation of a new phase component. The exact composition of an alloy and the casting condition will directly influence a kind and volume fraction of intermetallic phases [14-19]. Depending on the composition, the material may contain Al_2Cu , Mg_2Si , Al_2CuMg , and Si as well as $\text{Al}(\text{Fe},\text{M})\text{Si}$ particles, where M denotes such elements as Mn, V, Cr, Mo, W or Cu. During homogenization or annealing, most of the as-cast soluble particles from the major alloying additions such as Mg, Si and Cu is dissolved,

* DEPARTMENT OF MATERIALS SCIENCE, RZESZÓW UNIVERSITY OF TECHNOLOGY, 35-959 RZESZOW, 2 W. POLA STR. POLAND

and intermediate-sized 0.1 to 1 μm dispersoids of the Al-CuMgSi type, can form. Dispersoids can also result from the precipitation of Mn-, Cr-, or Zr-containing phases. A size and distribution of these various dispersoids depend on the time and temperature of the homogenization and/or annealing processes. Fine intermetallic particles ($<1 \mu\text{m}$) are formed during artificial aging of alloys and they are more uniformly distributed than constituent particles or dispersoids. The dimensions, shape and distribution of these particles may have also important influence on the ductility of alloys. Therefore, a systematic research is necessary regarding their formation, structure and composition.

For example, the coarse particles can influence the recrystallization, fracture, surface and corrosion, while the dispersoids control grain size and provide stability to the metallurgical structure. The dispersoids can also affect the fracture performance and may limit strain localization during deformation. The formation of particles drains solute from the matrix and, consequently, changes the mechanical properties of the material. This is particularly relevant to the heat-treatable alloys, where depletion in Cu, Mg, and Si can significantly change the metastable precipitation processes and age hardenability of the material [2,21-27]. Therefore, the particle characterization is essential not only for choosing the best processing routes, but also for designing the optimized alloy composition [15-18].

The main objective of this study was to analyze a morphology and composition of the complex microstructure of intermetallic phases in cast AlCu₄Ni₂Mg₂ aluminium alloy in T6 condition and consequently recommend the best experimental techniques for analysis of the intermetallic phases occurring in the aluminium alloys.

2. Material and methodology

The investigation was carried out on the Al-Cu₄Ni₂Mg₂ belonging to the 2xxx group casting aluminium alloys. The chemical composition of the alloy is: 4.3% Cu, 2.1% Ni, 1.5% Ni, 0.3% Zn, 0.1% Fe, 0.1% Si, Al bal [wt%]. The alloy was subjected to T6 heat treatment: solution heat treated at 520 °C for 5 h followed by water cooling and aging at 250 °C for 5 h followed by air cooling. The microstructure of examined

alloy was observed using an optical microscope – Nikon 300 on the polished sections etched in Keller solution (0.5 % HF in 5ml H₂O). The observation of specimens morphology was performed on the scanning electron microscope (SEM) HITACHI S-3400, operating at 6-10 kV in a conventional back-scattered electron mode and the transmission electron microscopes (TEM) Tesla BS-540 and Jeol-2100 operated at 120 and 200kV respectively. The thin foils were prepared by the electrochemical polishing in: 260 ml CH₃OH + 35 ml glycerol + 50 ml HClO₄ using Tenupol-3. The chemical composition of the intermetallics was made by energy dispersive spectroscopy (EDS) attached to the SEM manufactured by Thermo Noran.

The intermetallic particles from investigated Al-Cu₄Ni₂Mg₂ alloy were additionally extracted chemically in phenol. The samples in the form of disc were cut out from the rods of $\varnothing 12$ mm diameter. Then ~ 0.8 mm thick discs were prepared by two-sided grinding to a final thickness of approximately 0.35 mm. The isolation of phases was performed according to following procedure: 1.625 g of the sample to be dissolved was placed in a 300 ml flask containing 120 mm of boiling phenol (182 °C). The process continued until the complete dissolution of the sample occurred ~ 10 min. The phenolic solution containing the residue was treated with 100 ml benzyl alcohol and cooled to the room temperature. The residue was separated by centrifuging a couple of times in benzyl alcohol and then twice more in the methanol. The dried residue was refined in the mortar. After sieving of residue ~ 0.2 g isolate was obtained. The intermetallic particles from the powder extract were identified by using X-ray diffraction analysis. The X-ray diffraction analysis of the powder was performed using ARL-XTR'a diffractometer - Cu K radiation at 40 kV.

3. Results and discussion

The microstructure of investigated AlCu₄Ni₂Mg₂ alloy in T6 condition is shown in Figure 1. The analyzed microstructure consists different precipitates varied in shape, i.e.: fine sphere-like and strip-like (I), complex rod-like (II) and ellipse-like (III). The characteristics of these phases are presented in Table 1.

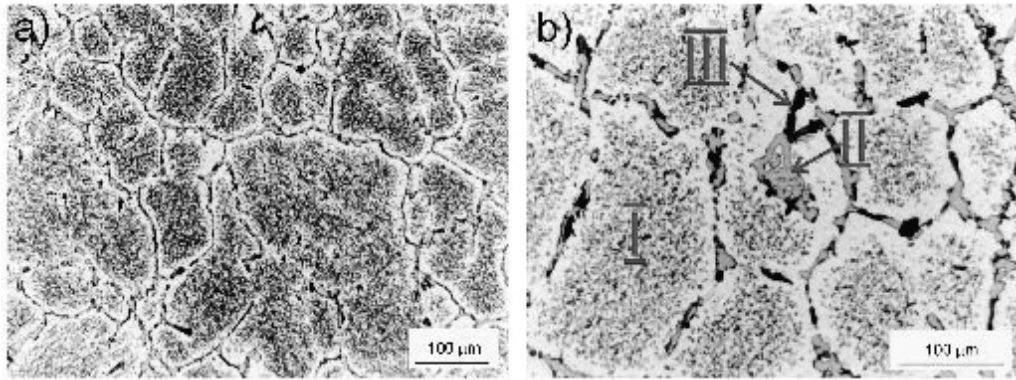


Fig. 1. Optical (Light) microscope image of the AlCu4Ni2Mg2 alloy in the T6 condition

TABLE 1

The characteristics of the phases in AlCu4Ni2Mg2 alloy

The characteristics		The phase number		
		I	II	III
Color	Unetched	–	Fair grey	Fair grey
	Etched	grey	Well shaped edges, the color changes into dark gray	The color changes into dark
Shape		Sphere-like and strip-like	Complex rod-like	Ellipse-like
Distribution		Homogeneous in the matrix of the α -Al alloy + small amount in the boundary zone	In the interdendritic areas of the α -Al alloy	In the interdendritic areas of the α -Al alloy

In order to identify the intermetallic phases in the examined alloy, series of elemental maps were performed for the elements line Mg-K, Al-K, Fe-K, Ni-K, Cu-K (Fig. 2). The maximum pixel spectrum clearly shows the presence of Ni and Cu in the scanned microstruc-

ture. In order to identify the presence of the elements in the observed phases, two regions of the mapped phase with high nickel and copper concentration were marked and their spectra evaluated.

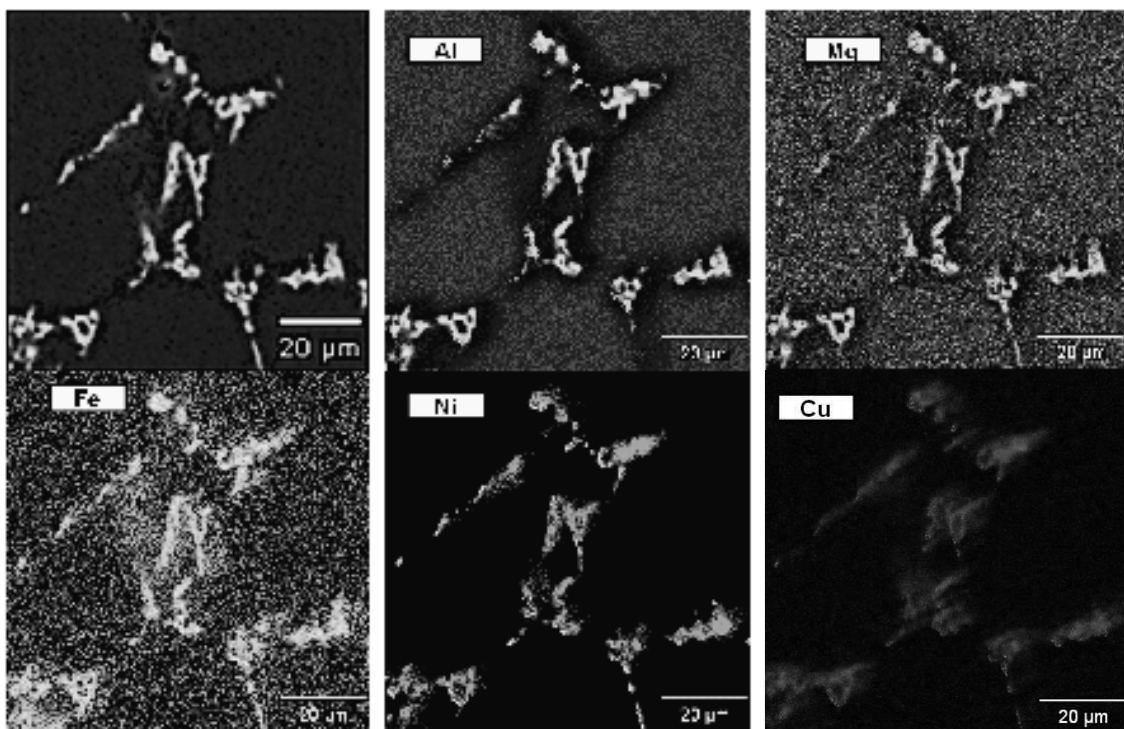


Fig. 2. SEM image of the AlCu4Ni2Mg2 alloy and corresponding elemental maps of: Al, Mg, Fe, Ni and Cu

As seen in the elemental maps in Fig. 2, the regions enriched in Ni and Cu correspond to the formation of type II precipitates (complex rod-like) and type III – ellipse-like precipitates observed in Figure 1. Figure 3 shows the scanning electron micrographs and EDS analysis

of particles in the investigated alloy. The EDS analysis performed on the phases present in microstructure of the alloy revealed, that complex rod-like phase (II) is the $\text{Al}_7\text{Cu}_4\text{Ni}$ one, whereas the ellipse-like (III) is $\text{Al}_3(\text{CuFeNi})_2$ (Fig. 3 and Tab. 2)

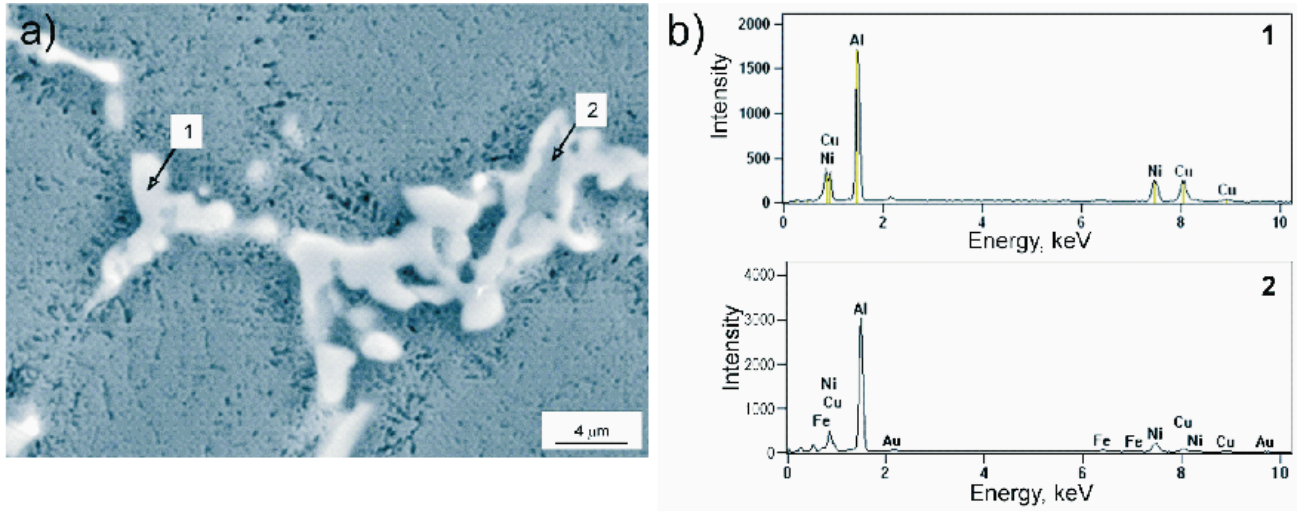


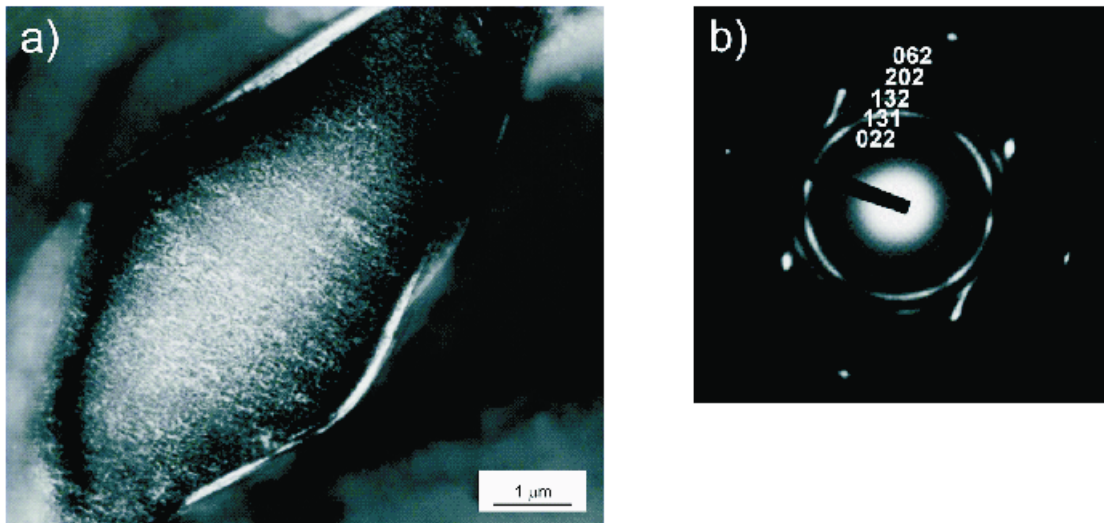
Fig. 3. a) SEM micrographs of the $\text{AlCu}_4\text{Ni}_2\text{Mg}_2$ alloy in the T6 condition; b) The corresponding EDS-spectra acquired in positions indicated by the number 1 and 2

TABLE 2

The chemical composition and volume fraction of the intermetallic phases in the $\text{AlCu}_4\text{Ni}_2\text{Mg}_2$ alloy

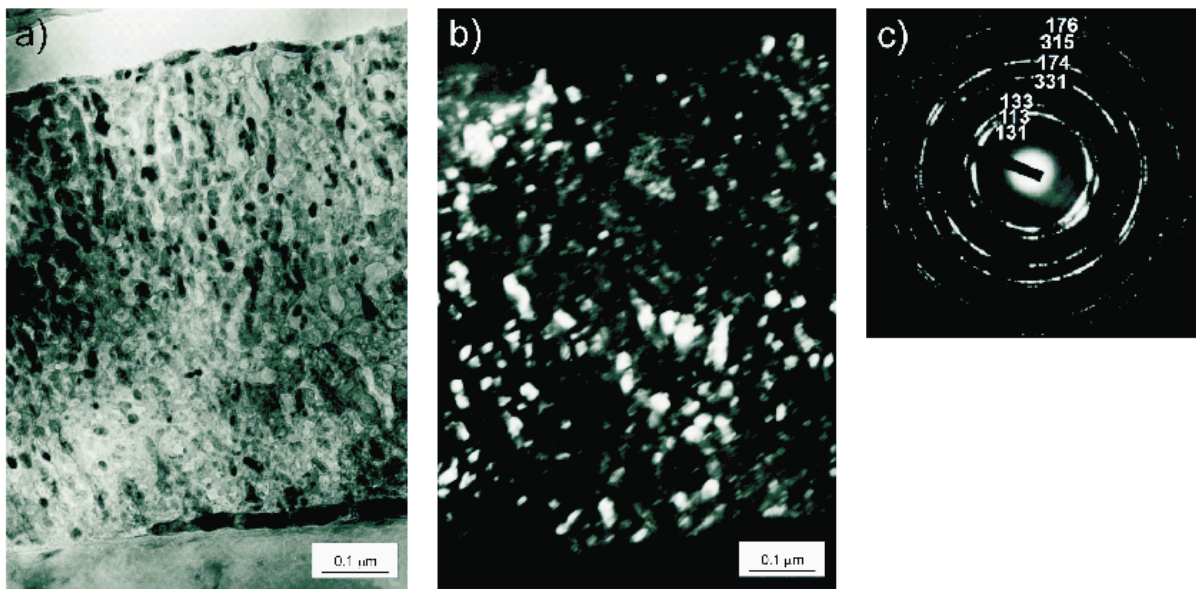
The phase number	Type of phases	Chemical composition of determined intermetallic phases (%at)	Volume fraction of the intermetallic phases in $\text{AlCu}_4\text{Ni}_2\text{Mg}_2$ alloy V_V [%]
I	Al_2Cu	–	–
II	$\text{Al}_7\text{Cu}_4\text{Ni}$	Al 52.9÷65.2 Cu 23.7÷30.2 Ni 7.1÷8.6	2.3
III	$\text{Al}_3(\text{CuFeNi})_2$	Al 65.9÷73.1 Cu 10.5÷19.3 Ni 7.1÷10.3 Fe 4.5÷7.5	1.1

The microstructure of the examined alloy $\text{AlCu}_4\text{Ni}_2\text{Mg}_2$ in T6 state consists of the primary precipitates of intermetallic phases combined with the highly dispersed particles of hardening phases. The TEM micrographs and the selected area electron diffraction patterns analysis proved that the dispersed precipitates showed in Fig. 1 and 2 are the intermetallic phases S- Al_2CuMg (Fig. 4 and 5) and Al_6Fe (Fig. 6) besides the precipitates of hardening phase $\theta\text{-Al}_2\text{Cu}$ were present in $\text{AlCu}_4\text{Ni}_2\text{Mg}_2$ alloy (Fig. 7).



h k l	022	131	132	202	062
Measured d (nm)	28.73	23.50	20.24	17.34	14.12
Standard d (nm): S-Al ₂ CuMg	28.29	13.13	20.18	17.49	14.16

Fig. 4. TEM micrograph of AlCu₄Ni₂Mg₂ alloy in T6 conditions showing the precipitate of the S-Al₂CuMg phase (a), and corresponding electron diffraction pattern (b)



h k l	131	113	133	331	174	315	176
Measured d (nm)	22.86	19.77	17.07	12.06	10.25	9.83	8.53
Standard d (nm): S-Al ₂ CuMg	23.12	20.00	17.06	12.09	10.27	9.71	8.64

Fig. 5. TEM micrograph of AlCu₄Ni₂Mg₂ alloy in T6 conditions showing the precipitate of the S-Al₂CuMg phase (a), and corresponding electron diffraction pattern (b)

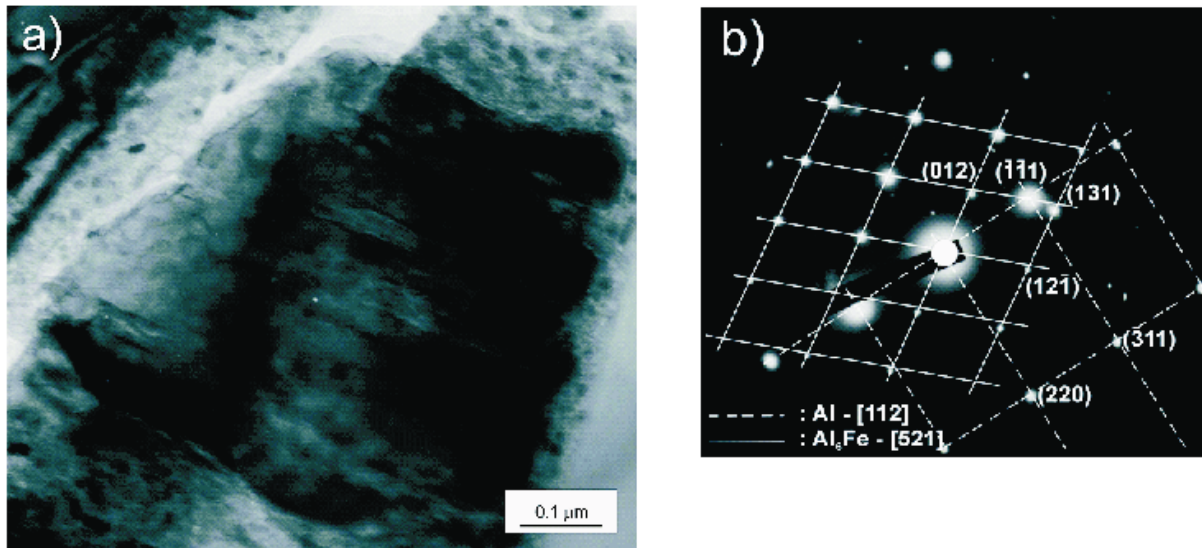


Fig. 6. TEM micrograph of AlCu4Ni2Mg alloy in T6 condition showing the precipitate of the Al₆Fe phase (a), and corresponding electron diffraction pattern (b)

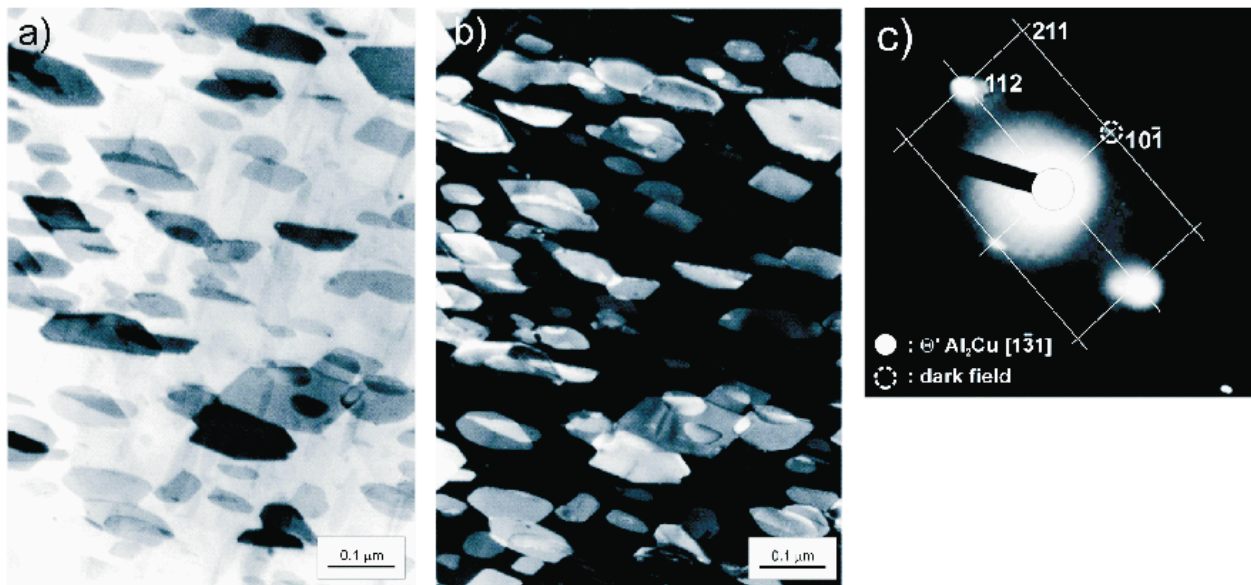


Fig. 7. TEM micrograph of AlCu4Ni2Mg alloy in T6 condition showing the precipitates of hardening phase θ' -Al₂Cu: strip-shaped (a), compact-shaped (b)

The presented above results were compared with those obtained for the particles extracted from the Al-Cu₄Ni₂Mg₂ alloy using phenolic dissolution technique. The particles have irregular shape (Fig. 8). The EDS spectra revealed the presence of Al, Cu, Fe and Ni – bearing particles in the extracted powder (Fig. 8 b and d). The EDS analysis results presented in Table 3 proof that analyzed particles are Al₇Cu₄Ni and Al₃(CuFeNi)₂.

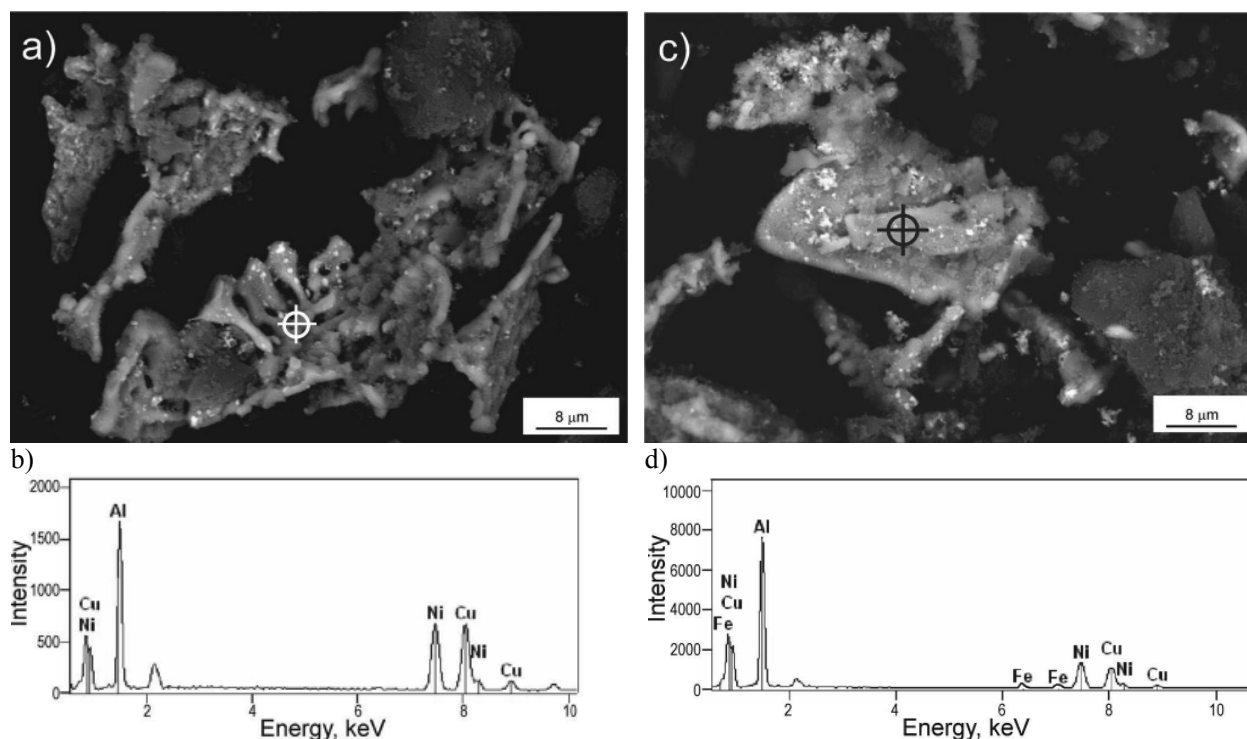


Fig. 8. SEM micrographs (a,c) and EDS spectra (b,d) of the particles extracted from the AlCu₄Ni₂Mg₂ alloy

TABLE 3

The chemical composition of the intermetallic phases extracted from the AlCu₄Ni₂Mg₂ alloy

Chemical composition of intermetallic phases (%at)		Type of phases
The phase from Fig. 8a	Al 51.4÷64.82 Cu 22.9÷29.3 Ni 7.5÷8.9	Al ₇ Cu ₄ Ni
The phase from Fig. 8c	Al 66.1÷72.9 Cu 10.1÷19.6 Ni 6.9÷10.8 Fe 4.4÷7.8	Al ₃ (CuFeNi) ₂

The results of the SEM/EDS analysis of the particles extracted with boiling phenol from AlCu₄Ni₂Mg₂ alloy were compared with X-ray diffraction pattern (Fig. 9).

The observed peaks confirmed SEM and TEM results. The majority of the peaks were from Al₇Cu₄Ni, Al₆Fe, S-Al₂CuMg, and Al₃(CuFeNi)₂.

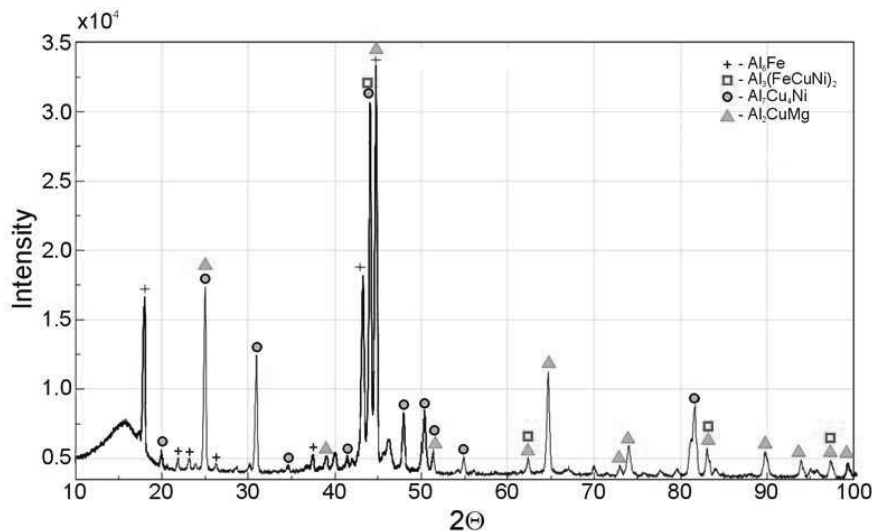


Fig. 9. The X-ray diffraction from the particles extracted from AlCu₄Ni₂Mg₂ alloy

On the other hand, it is nearly impossible to make unambiguous identification of the all intermetallics present in an aluminium alloy which are rather complex, even applying all well-known experimental techniques. X-ray diffraction analysis is one of the most powerful and appropriate technique giving the possibility to determine most of verified intermetallics based on their crystallographic parameters. Our analysis shows that the difficulties of having reliable results of all the possible existing phases in a microstructure of the alloy is related to the procedure of phase isolation. The residue is separated by centrifuging and since some of the particles are very fine and available sieves are having too big outlet holes there is no chance prevents them from being flowing out from a solution.

4. Conclusions

Currently, efforts are being directed towards the development of analytical techniques which rapidly achieve an accurate determination of phase components in an alloy. The obtained results revealed that the phenol extraction method is an alternative to the other techniques applied to phase identification. This method was successfully applied to the AlCu₄Ni₂Mg₂ aluminium alloy. The main advantages of dissolution techniques are its reliability – when used properly you will always get pure residue – and its low price. The major disadvantages of phenol extraction method are the possible contamination of the residue and the time needed.

The examined alloy in T6 condition possessed a complex microstructure. By using various instruments and techniques (LM, SEM-EDS, TEM and XRD) a wide range of

intermetallics phases were identified. The microstructure of investigated alloys in T6 condition included five phases, namely: Al₇Cu₄Ni, θ-Al₂Cu, Al₆Fe, S-Al₂CuMg, and Al₃(CuFeNi)₂.

Acknowledgements

This work was carried out with the financial support of the Ministry of Science and Higher Education under grant No. **PBZ-MNiSW-3/3/2006**

REFERENCES

- [1] P. Hodgson, B. A. Parker, *Journal of Materials Science* **16**, 1343-1348 (1981).
- [2] K. Sato, I. Izumi, *Materials Characterization* **37**, 61-80 (1985).
- [3] A. K. Gupta, P. H. Marois, D. J. Lloyd, *Materials Characterization* **37**, 66-80 (1996).
- [4] *Aluminium Handbook*. vol.1 Fundamentals and materials. Aluminium-Verlag Marketing & Kommunikation GmbH, Düsseldorf 1999.
- [5] G. soGustafsson, T. Thorvaldsson, G. L. Dunlop, *Metallurgical and Materials Transactions* **17A**, 45-52 (1986).
- [6] F. King, *Aluminium and its alloys*. John Wiley & Sons, New York-Chichester-Brisbane-Toronto, 1987.
- [7] L. F. Mondolfo, *Aluminium Alloys: Structure and Properties*. Butterworths, London-Boston, 1976.
- [8] Y. L. Liu, S. B. Kang, H. W. Kim, *Materials Letters* **41**, 267-272 (1999).
- [9] J. W. Martin, *Precipitation Hardening*. Oxford, Pergamon Press, 1968.
- [10] I. J. Polmear, *Light alloys*. Metallurgy of the light metals. Arnold, London-New York-Sydney-Auckland, 1995.

- [11] L. A. Dobrzański, R. Maniara, M. Krupiński, J. H. Sokolowski, *Journal of Achievements in Materials and Manufacturing Engineering* **24**, 51-54 (2007).
- [12] M. Kciuk, S. Tkaczyk, *Journal of Achievements in Materials and Manufacturing Engineering* **21**, 39-42 (2007).
- [13] M. Takeda, A. Komatsu, M. Sohta, T. Shirai, T. Endo, *Scripta Materialia* **39**, 1295-1300 (1998).
- [14] M. Warmuzek, G. Mrówka, J. Sieniawski, *Journal of Materials Processing Technology* **157-158**, 624-632 (2004).
- [15] S. Zajac, B. Bengtsson, C. Jönsson, *Materials Science Forum*, 396-402 (2002) 399-404.
- [16] G. Mrówka-Nowotnik, J. Sieniawski, M. Wierzbińska, *Archives of Materials Science and Engineering* **28**, 69-76 (2007).
- [17] G. Mrówka-Nowotnik, J. Sieniawski, M. Wierzbińska, *Journal of Achievements in Materials and Manufacturing Engineering* **20**, 155-158 (2007).
- [18] M. Wierzbińska, G. Mrówka-Nowotnik, *Archives of Materials Science and Engineering* **30**, 85-88 (2008).
- [19] L. A. Dobrzański, R. Maniara, J. H. Sokolowski, *Journal of Achievements in Materials and Manufacturing Engineering* **17**, 217-220 (2006).
- [20] R. A. Siddiqui, H. A. Abdullah, K. R. Al-Belushi, *Journal of Materials Processing Technology* **102**, 234-240 (2000).
- [21] G. Sha, K. O'Reilly, B. Cantor, J. Worth, R. Hamerton, *Materials Science and Engineering* **A304-306**, 612-616 (2001).
- [22] A. K. Gupta, D. J. Lloyd, S. A. Court, *Materials Science and Engineering* **A316**, 11-17 (2001).
- [23] M. Warmuzek, K. Rabczak, J. Sieniawski, *Journal of Materials Processing Technology* **162-163**, 422-428 (2005).
- [24] M. Warmuzek, J. Sieniawski, K. Wicher, G. Mrówka-Nowotnik, *Journal of Materials Processing Technology* **175**, 421-426 (2006).
- [25] J. A. Garcia-Hinojosa, C. R. Gonzalez, Y. Houbert, *Journal of Materials Processing Technology* **143-144**, 306-310 (2003).
- [26] M. Wierzbińska, J. Sieniawski, *Journal of Achievements in Materials and Manufacturing Engineering* **14**, 31-35 (2006).
- [27] L. Dobrzański, W. Borek, R. Maniara, *Journal of Achievements in Materials and Manufacturing Engineering* **18**, 211-214 (2006).

